

Dose dependency of outcomes of intrapleural fibrinolytic therapy in new rabbit empyema models

Andrey A. Komissarov^{‡§*}, Galina Florova^{‡*}, Ali O. Azghani¹, Ann Buchanan[‡], Jake Boren[‡], Timothy Allen², Najib M. Rahman³, Kathleen Koenig[‡], Mignote Chamiso[‡], Sophia Karandashova[‡], James Henry[‡] and Steven Idell[‡]

[‡] The Department of Cellular and Molecular Biology of the University of Texas Health Science Center at Tyler, 11937 US Highway 271, Tyler, TX 75708-3154, USA; ¹The University of Texas at Tyler, Tyler, TX; ² Department of Pathology, The University of Texas Medical Branch, Galveston, TX; ³ Oxford Centre for Respiratory Medicine, Oxford University Hospitals, NHS Trust, Oxford, UK;

Running head: Fibrinolytic therapy in rabbit empyema

* These authors contributed equally to this work

§ Address correspondence to:

Andrey Komissarov Ph.D.,
Associate Professor of Biochemistry
The University of Texas Health Science Center at Tyler
11937 US Highway 271
Lab C-6, Tyler, TX 75708
USA; phone: 903 877 5183
Fax: 903 877 5627;
Email: andrey.komissarov@uthct.edu

Supported by: NIH 1 P50 HL107186 CADET I and The Texas Lung Injury Institute

24 **Key words:** Empyema, fibrinolysis, tissue plasminogen activator, single chain urokinase,
25 plasminogen activator inhibitor-1

26 Conception and design: GF, AAK, SI; Acquisition, analysis and interpretation: AAK, GF, TA,
27 AOA, SI; NMR, JB, AB, JH, KK, SK, MC Drafting the manuscript for important intellectual
28 content: SI, GF, AAK.

29

Abstract

The incidence of empyema (EMP) is increasing worldwide, generally occurs with pleural loculation and impaired drainage is often treated with intrapleural fibrinolytic therapy (IPFT) or surgery. A number of IPFT options are used clinically with empiric dosing and variable outcomes in adults. To evaluate mechanisms governing intrapleural fibrinolysis and disease outcomes, models of *Pasteurella multocida* and *Streptococcus pneumoniae* were generated in rabbits and the animals were treated with either human tissue (tPA) plasminogen activator or prourokinase (scuPA). Rabbit EMP was characterized by the development of pleural adhesions detectable by chest ultrasonography and fibrinous coating of the pleura. Similar to human EMP, rabbits with EMP accumulated sizable; 20-40 ml fibrinopurulent pleural effusions associated with extensive intrapleural organization, significantly increased pleural thickness, suppression of fibrinolytic and plasminogen activating activities and accumulation of high levels of plasminogen activator inhibitor 1, plasminogen and extracellular DNA. IPFT with tPA (0.145 mg/kg) or scuPA (0.5 mg/kg) was ineffective in rabbit EMP (n=9 and 3 for *P. multocida* and *S. pneumoniae*, respectively). 2 mg/kg tPA or scuPA IPFT (n=5) effectively cleared *S. pneumoniae* induced EMP collections in 24h with no bleeding observed. While intrapleural fibrinolytic activity for up to 40 min after IPFT was similar for effective and ineffective doses of fibrinolysin, it was lower for tPA than for scuPA treatments. These results demonstrate similarities between rabbit and human EMP, the importance of pleural fluid PAI-1 activity and levels of plasminogen in the regulation of intrapleural fibrinolysis and illustrate the dose dependency of IPFT outcomes in EMP.

Introduction

Intrapleural fibrinolytic therapy (IPFT) has been used to treat patients with organizing pleural injury that generally occurs in patients with empyema (EMP) or complicated parapneumonic pleural effusions. In these and preclinical situations, pleural fluid biomarkers such as decreased pH, high levels of plasminogen activator inhibitor-1 (PAI-1) and the detection of bacterial organisms are indicative of a propensity towards loculation, difficult drainage and poor clinical outcomes (6; 16; 31; 40). While IPFT has been used for over sixty years (37; 38), clinical dosing remains entirely empiric(7; 8) and there is no currently FDA-approved form of IPFT or, to our knowledge , by any international regulatory body. The dosing of tPA-based IPFT varies from 10-100 mg/unit dose (36), while the dose of intrapleural tPA used in the MIST2 trial was 10 mg with or without supplemental DNase was likewise empiric (34). How pleural fluid components, dosing of IPFT and interactions of the components with the intrapleurally delivered fibrinolysins affect treatment outcomes and how fibrinolysins are processed in EMP is to our knowledge unknown, raising the possibility that empiric, uniform clinical dosing is suboptimal. These considerations motivated us to create an animal model in which these gaps in current knowledge could be addressed and in which therapeutics designed for human use could be tested.

It is now clear that pleural organization in EMP evolves with early formation of fibrinous pleural adhesions (16-18) followed by pleural thickening attributable to proliferation of myofibroblasts (10; 11) and neomatrix deposition ultimately leading to pleural loculation that impedes pleural drainage. These changes predispose to persistent sepsis and lung restriction (16). Intrapleural fibrin deposition is initiated via an accelerated procoagulant response and maintained by local elaboration of inhibitors, in particular PAI-1 (16). PAI-1 is overexpressed in human and preclinical pleural injury, is increased in pleural fluids (16; 19), can increase the severity of organization when overexpressed in the pleural compartment (23) and inhibits the

activity of either tissue plasminogen activator (tPA) or two chain urokinase or prourokinase; single chain urokinase (scuPA)-based IPFT (23). In addition, PAI-1 targeting expedites the resolution of organizing pleural injury induced by tetracycline in rabbits and permits the use of attenuated doses of fibrinolysins (13). We have previously shown that the rabbit model is advantageous for analysis of the safety and effects of IPFT designed for human use, given the similarity of the interactions between rabbit and human fibrinolysins and inhibitors (21; 26). Because we previously used models of tetracycline and *P. multocida*-induced with limited pleural organization in rabbits (13; 18; 20; 23-25), we inferred that development of a novel model of EMP that recapitulated the organizational progression and sequestration of pleural fluid was possible. We therefore sought to generate a model of *S. pneumoniae*-induced EMP in rabbits, as this is a common cause of the clinical disease, because the relatively large size of the animal facilitates the testing of IPFT and the rabbit model is tractable for trended imaging of the chest by ultrasonography (25). We also adapted the *P. multocida* EMP model so that pleural adhesions simulating loculae developed. We characterized the models and then used them to assess the role of PAI-1 to regulate pleural injury outcomes, define processing of two plasminogen activators; tPA or scuPA to alter injury outcomes and test their ability to clear pleural organization and enhance drainage.

Materials and Methods

Empyema Models — The *Institutional Animal Care and Use Committee* at the University of Texas Health Science Center at Tyler approved the animal protocol under which animals were utilized in this study. New Zealand, white, pathogen free, female rabbits (weight= 3.0 to 3.6 kg; average age 18 weeks, were used in this study and were obtained from Charles River (Wilmington, MA). A total of 44 rabbits were used in this study. EMP was induced by intrapleural injection of 1×10^8 cfu of *S. pneumoniae*, D39 strain, *National Collection of Type Cultures*,

Salisbury UK delivered in a 3 ml of 0.5% brain heart infusion agar into the right pleural space. In an alternative model, *P. multocida* was given intrapleurally at the same inoculation dose. *P. multocida* (ATCC 7228) was obtained from American Type Culture Collection. Antibiotic treatment (Clavomox) 10 mg/kg to which the *S. pneumoniae* and *P. multocida* strains were susceptible) was initiated 18h post infection and was administered daily by subcutaneous injection for 2-4d. No chest tube was placed, as this is difficult to maintain and drainage via the tube blocks formation of pleural adhesions. After intrapleural inoculation, rabbits were continuously monitored around the clock to monitor temperature, SpO₂, activity and behavior. Fluids (100 ml of warmed 0.9% Saline solution) were delivered subcutaneously every 24h. Ultrasonography was used daily starting at 24h to monitor development of the model and pleural fluid accumulation. Anesthesia, post-operative pain medication, and animal care were provided as previously reported (23). No animals were moribund or required euthanization. After delivery of the organisms, rabbits were individually housed throughout the course of the experiment.

Rabbits with EMP were treated with either intrapleural tPA, scuPA or vehicle control PBS (sterile phosphate buffered saline), with a single intrapleural dose of IPFT given at 72h post induction of pleural injury, as previously reported (18; 24). tPA at a dose of either [0.145 mg/kg, the minimal effective dose (MED) in rabbits with tetracycline (TCN)-induced pleural injury, or 2 mg/kg], scuPA (0.5 mg/kg, TCN MED or 2 mg/kg) or vehicle control was administered intrapleurally using an 18 gauge, 1.25 long Excel Safelet Catheter, which was then cleared using 0.5 ml of PBS. 0.5 ml aliquots of pleural fluid were collected at 10, 20 or 40 min after IPFT. After collection, samples were immediately centrifuged, citrated, and snap frozen (23; 24). Cell-free samples were stored at -80°C and subsequently analyzed. Rabbits were carefully monitored for signs of pain, discomfort, or distress to ensure animal stability and wellbeing. If tachypnea developed, the animals were subjected to chest ultrasonography with removal of 20 cc of pleural fluid by thoracentesis done under sedation and local infiltration with 2 percent lidocaine,

which was only required in some animals. Euthanasia was accomplished at 96h by intravenous administration of Beuthanasia D (1 ml), followed by exsanguination via the aorta after which pleural fluid was collected and processed as described above and the pleural cavity was harvested and fixed. A small volume of pleural fluid collected for immediate analysis was kept at room temperature and continuously agitated until analysis was complete. The total red blood cell and white blood cell counts in pleural fluids were measured using an automated Coulter Counter (Coulter Electronics, Luton, UK). Cytospin slides were prepared for differential white blood cell counts and stained using the Hema 3 ® Stain Set (Fisher Diagnostics, Waltham, MA), following the manufacturer's protocol.

Ultrasonography — B-mode ultrasonography of the chest was performed as described elsewhere (24) using Logiq e system (GE Healthcare, Milwaukee, WI), equipped with R5.2.x software and a multi-frequency transducer model 12L-RS (3-10.0 MHz) at a working frequency of 10 MHz, as we previously reported (25).

Metrics of Pleural Injury — Gross Loculation Injury Scores (GLIS) were calculated for each animal as described (23; 25). IPFT was considered successful based upon a GLIS<10. Multiple visceral-parietal interconnected fibrin webs and sheets or “too numerous to count” strands and fibrinous lung coating correlated with a GLIS=50. Pleural thickness was measured by morphometry, as we previously reported (40).

Human Pleural Fluids — Pleural fluids from patients enrolled in the MIST2 trial were citrated, collected and archived by Dr. Rahman. The fluids were collected from patients with pleural infection, some of whom were loculated and other with free-flowing pleural fluids when enrolled in the study. Pleural fluids were also prospectively collected from patients with EMP at UTHSCT, mainly from the surgery service at the time of VATS or open drainage. All studies were approved by the MIST2 participant institution and UTHSCT institutional human subjects

review boards, respectively. Pleural fluids were collected and stored at -70°C until processed as we previously reported (19).

Fibrinolytic and Plasminogen Activation Activities in Pleural Fluids of Animals Treated with IPFT — Measurements of the PA activity of uPA and tPA in rabbit pleural fluids were carried out and analyzed as previously described (27). Fibrinolytic activity was measured as we previously reported (26). Plasminogen activation assays were performed as previously described (29).

PAI-1 Activity Assay — Levels of active and total rabbit PAI-1 in the pleural fluids were determined by ELISA (Molecular Innovations, Novi, MI).

Data Analysis and Statistics — Levels of statistical significance were determined using Kruskal-Wallis test and pairwise multiple comparison procedures (Holm-Sidak method and Turkey Test). Data analysis was performed using SigmaPlot 12.0 for Windows (SPSS Inc.), as previously described (19). Correlation coefficients (r) calculated from curve fittings were used as a parameter of the exactness of the fit ($r^2 > 0.90$ for all the kinetic data).

Results

Characterization of the *P. multocida* and *S. pneumoniae*-induced EMP in rabbits. Both *P. multocida* and *S. pneumoniae*-induced EMP were characterized by the development of pleural adhesions that were detectable by chest ultrasonography *in vivo* and fibrinous coating that diffusely covered the entirety of the visceral right hemithorax in which EMP was induced (Figure 1, Panels A and B). As opposed to the ease with which pleural fluids were readily aspirated from rabbits at 96h after TCN-induced pleural injury, as we previously reported (18; 18; 21; 27), pleural fluids from both *P. multocida* and *S. pneumoniae*-induced EMP were difficult to aspirate at the time of sacrifice, in part attributable to the extensive pleural organization that was present

(Figure 1, Panels A and B) and to the grossly purulent character of the pleural fluids. In some areas, organizing fibrinous collections in each EMP model assumed a locular, rounded appearance and appeared to sequester pleural fluids, resembling the loculations found in human EMP. Pleural thickening was readily detectable by histologic analyses in both *P. multocida* and *S. pneumoniae*-induced EMP by 96h post infection (Figure 1, bottom left panels). By Trichrome staining (Figure 1, lower middle panels), the transitional fibrin neomatrix appeared to be organizing with formation of a collagenous visceral pleural rind by 96h post-infection in both models. The fibrinous character of the submesothelial visceral pleural thickening was confirmed by immunohistochemistry (Figure 1, lower right panels), and fibrinous strands were detected, best visualized in the *S. pneumoniae* model in the figure. The *P. multocida* EMP-injured animals typically had increased inflammation at the visceral pleural surface. All animals with EMP induced by either *S. pneumoniae* or *P. multocida* had peripheral pneumonitis within the lung parenchyma that was associated with induction of EMP.

Characterization of EMP pleural fluids. Pleural injury in both *P. multocida* and *S. pneumoniae* EMP models resulted in accumulation of significant amounts (20-40 ml) of pleural fluid, which recapitulated grossly purulent character of human EMP fluids. The levels of active and total PAI-1 in pleural fluids of rabbits with *P. multocida* and *S. pneumoniae* EMP were elevated, with levels that were comparable to those observed in pleural fluids from patients with EMP (Figure 2). Fibrinolytic activity was undetectable in EMP fluids from rabbits at 96h after induction of EMP by either *P. multocida* or *S. pneumoniae* (Figure 3). However, supplementation of these same pleural fluids with exogenous fibrinolysin resulted in activation of the endogenous plasminogen and resulted in significant increases in the fibrinolytic activity of EMP fluids from both models (Figure 3). Notably, similar changes in fibrinolytic activity were observed in baseline; pretreatment, pleural fluids of patients who were enrolled in the MIST2 trial of IPFT after supplementation with fibrinolysin (Figure 3). These observations demonstrate

that fibrinolytic activity in EMP fluids is at least in part suppressed by the elevated levels of PAI-1 they contain (Figure 2) and that the augmentation of plasminogen activator activity in amounts sufficient to overcome largely PAI-1-mediated PA inhibition generates readily detectable levels of fibrinolytic activity in rabbit pleural fluids, comparable to those observed in human EMP fluids. Such accumulation of plasminogen in pleural fluids was previously observed in rabbits with TCN-induced pleural injury and in humans with EMP (13). Infectious pleural injury in humans results in accumulation of the extracellular DNA in pleural fluids, which could affect the regulation of fibrinolysis within the pleural compartment (26). As anticipated, the intrapleural concentration of DNA in pleural fluids of rabbits with *P. multocida* and *S. pneumoniae* EMP was elevated and approached levels observed in EMP pleural fluids from humans (Figure 4) (26). The elevated white blood cell counts (WBCs) in pleural fluids averaged at 5×10^7 and 1.5×10^7 for *P. multocida* and *S. pneumoniae* models respectively, while differential analysis of WBC showed predominance of neutrophil population in the *S. pneumoniae* model at 96h with a more mixed myeloid cell population at the same interval after *P. multocida*-induced EMP (Figure 5). The pleural fluids were sterile at 96h in both EMP models. No apparent local or systemic bleeding was associated with either of the models and pleural fluid red blood cell counts were comparable in all models (data not shown). The concentration of total protein in pleural fluids in both rabbit EMP models ranged from 35-60 mg/ml. Thus, pleural fluids of both *P. multocida* and *S. pneumoniae* rabbit EMP models recapitulate several key features present in pleural fluids from human EMP.

IPFT with Minimal Effective Doses of either tPA or scuPA, determined in the model of TCN-induced pleural injury, was ineffective in rabbit EMP. The elevated levels of PAI-1 in pleural fluids (Figure 2) raised the possibility that doses of IPFT we previously defined as effective in chemically; TCN-induced pleural injury might be ineffective in rabbits with EMP. To test this possibility, we first used IPFT with MEDs of scuPA and tPA identified previously in

TCN-induced pleural injury in rabbits (18; 24). Rabbits with *P. multocida* (n=18) EMP were initially used in these experiments and were treated at 72h with intrapleural administration of a single TCN MED dose of 0.5 mg/kg scuPA or 0.145 mg/kg tPA (n=9/group). The results of IPFT were evaluated at 96h, as previously described (13; 24; 25) by GLIS scoring of the extent of pleural injury. Vehicle control animals (n=5) were treated with intrapleural PBS vehicle. Outcomes of IPFT and severity of the pleural injury in the *P. multocida* EMP groups treated with fibrinolysins were comparable to those observed in control untreated animals, as evaluated by GLIS (Figure 6), and morphometric analyses of pleural thickness (Figure 7). Based on these results and in order to conserve animals, we next tested the same TCN MED doses of scuPA or tPA in *S. pneumoniae*-induced EMP (n=3 rabbits/group). A total of 5 animals treated with intrapleural PBS served as controls as well. The TCN MED dose of tPA was ineffective, whereas partial clearance of pleural organization was observed when rabbits with EMP induced by *S. pneumoniae* EMP were treated with scuPA IPFT (Figure 6). There was no significant difference in pleural thickness of animals treated with these doses of tPA or scuPA in either model (Figure 7). Thus, the initial MED of both fibrinolysins, defined in a model of TCN-induced pleural injury (18; 24), were ineffective in treatment in both models of rabbit infectious EMP models (Figure 6; 7).

Changes in the PA and fibrinolytic activities in pleural fluids of rabbits treated with MEDs of tPA and scuPA derived from the TCN-induced model of pleural injury. While both tPA and scuPA progressively lost activity in EMP fluids during IPFT, PA activity was detectable for up to 40 minutes after intrapleural administration of each fibrinolysin (Figure 8). Thus, similar to TCN-induced pleural injury in rabbits, the minimal time of effective fibrinolysis (TEF) (25) in rabbit EMP is at least several hours (13; 24; 25) and 40 min of sustained PA activity alone is insufficient to clear intrapleural fibrin accumulated in either *P. multocida* or *S. pneumoniae* EMP in rabbits. Both PA and fibrinolytic activities were suppressed prior to IPFT and at the end of the

experiment (Figure 8; 0 and Final, respectively) and were significantly lower ($P<0.05$) than those observed at 10-40 min after IPFT (Figure 8). Similar responses of b-fibrinolytic and PA activities and to supplementation of pleural fluids with tPA (Figure 3) was previously observed in TCN-induced pleural injury in rabbits and in human pleural fluids prospectively collected at UTHCT, as previously reported (13). While both of the MEDs of scuPA and tPA were equally ineffective in the treatment of *P. multocida*-induced EMP (Figure 6A), rabbits with *S. pneumoniae* EMP treated with a MED of scuPA demonstrated improved (lower) GLIS scores than those treated with MED of tPA (Figure 6B). Moreover, intrapleural PA (Figure 8) and fibrinolytic (Figure 9) activities during the first 40 min of IPFT of *S. pneumoniae* EMP appeared to be higher in animals treated with a MED of scuPA, compared to those that received tPA (Figures 8,9), which coincided with the better scuPA GLIS outcome (Figure 6) and changes in pleural thickness (Figure 7C). Higher PA activity in pleural fluids of scuPA treated animals (Figure 8) was likely due to the higher dose of the fibrinolysin (MED for scuPA and tPA are 0.5 and 0.145 mg/kg, respectively (18)). However, higher fibrinolytic activity after scuPA treatment (Figure 9) could reflect a different intrapleural mechanism governing its regulation in EMP. Since a higher dose of a fibrinolysin (0.5 mg/kg of scuPA) resulted in a better GLIS outcome in treatment of *S. pneumoniae* EMP (Figure 6), we hypothesized that a further increase in the dose of the fibrinolysins could result in more effective IPFT outcomes in either *S. pneumoniae* or *P. multocida* EMP in rabbits.

A high dose (2 mg/kg) of tPA or scuPA effectively clears pleural organization in *S. pneumoniae*-induced EMP. In the further interest of conserving animals and with comparable results in both models using lower doses of the fibrinolysins, we opted to use the *S. pneumoniae* model to see if dose escalation would effectively clear pleural adhesions and fibrinous deposits. The IPFT dose of 2 mg/kg exceeds the MED for the TCN-model for scuPA and tPA by 4 and 13.8 fold, respectively and was previously shown to be effective and tolerated

in rabbits with TCN-induced pleural injury (18). Rabbits with *S. pneumoniae* EMP were treated with intrapleural injection of 2.0 mg/kg of scuPA (n=5) and tPA (n=5) and outcomes of IPFT were analyzed in 24h as previously described (13; 24; 25). In a control group (n=5), the animals were treated with intrapleural administration of a dose of the interventional agent vehicle (PBS). In contrast to IPFT in which the MEDs for either tPA or scuPA were used (Figure 6), administration of 2 mg/kg of either agent resulted in effective therapy (GLIS<10) (Figure 10). Favorable outcomes of IPFT were confirmed by ultrasonography, gross and microscopic evaluations (Figure 10 A-E). Thus, the 2 mg/kg dose of both fibrinolysins was well-tolerated and effective for treatment of *S. pneumoniae* EMP. Notably, despite the higher intrapleural PA activity observed for both fibrinolysins during first 40 min of IPFT (Figure 11A, B), the profiles of intrapleural fibrinolytic activity (Figure 10C, D) were similar to those observed with treatment with an ineffective, lower doses of fibrinolysins in *S. pneumoniae*-induced EMP (Figure 9C, D), indicating the importance of the longer half-life of the PA activity for successful IPFT (13; 25). Similar to the results observed when animals were treated with MEDs of scuPA and tPA (Figure 9), the fibrinolytic activity in pleural fluids of animals treated with scuPA was significantly higher than that for animals treated with tPA (Figure 11C, D), indicating differences in the mechanisms of intrapleural fibrinolysis in EMP for two fibrinolysins. On the other hand, both fibrinolytic and PA activities in several final samples were higher with 2 mg/kg dose (Figure 11) than those in ineffective doses (Figures 8C, D and 9C, D). Thus, an increase in the dose of the fibrinolysins resulted in a successful IPFT in *S. pneumoniae* EMP in rabbits, most likely due to an increase in the intrapleural half-life of the fibrinolysins. These results demonstrate the dose dependence of the outcomes of IPFT with two different fibrinolysins (human tPA and scuPA) in a rabbit model of *S. pneumoniae*-induced EMP.

Discussion

The newly characterized rabbit *S. pneumoniae* EMP model we now report offers substantive advantages, in that progressive pleural organization involves both formation of extensive pleural adhesions, loculae-like structures and pleural thickness. These changes were associated with impaired pleural drainage by thoracentesis by 96h and the development of peripheral pneumonitis after initiation of *S. pneumoniae* or *P. multocida*-induced EMP. These comprise important morphologic features, as clinical loculation impairs pleural drainage in patients with EMP and is associated with increased morbidity (16; 40). Increased pleural thickness has likewise been associated with poor outcomes of IPFT in these patients (1; 3). Fibrinous coating of the pleural surfaces with adhesion formation was observed over 72h of EMP in both models (Figure 1). As expected, chest ultrasonographic imaging can be used to follow the evolution of EMP over time, as we recently reported in rabbits with TCN-induced pleural injury (25).

In a previous study, we found that chest tube placement facilitated survival in rabbits with *P. multocida*-induced EMP, in which pleural thickening was present but pleural adhesions did not form because pleural fluid was routinely evacuated to promote survival (20). In the *P. multocida* EMP model we adapted for use in this study, tube thoracostomy was not done, allowing EMP fluids to remain in the chest and organize. Over 96h, there was comparable pleural organization that occurred in both *S. pneumoniae* or *P. multocida*-induced EMP, indicating that comparable pleural remodeling occurs with different infectious insults as may occur in human EMP. While the models are labor-intensive and entail round the clock care for at least 96h, all animals subjected to this protocol survived allowing for analysis of the pleural changes associated with progressive EMP.

Another advantage of the rabbit models is the proximity of the rabbit fibrinolytic system to that of humans. While murine EMP models (41) are attractive due to the availability of animals with different genetic backgrounds they possess inherent limitations for studies of fibrinolysis (9). Murine PAI-1 (12), fibrin (33), and urokinase receptor, uPAR (22) structurally and functionally differ from those of the human proteins. These differences could affect the translation of any findings in the murine models to humans. Fibrinolytic proteins in rabbits bear a closer resemblance to those in humans, suggesting these animals are more suitable for studies of IPFT with human PAs. Rabbit plasminogen is readily cleaved to active plasmin by either intrapleurally administered human tPA, two chain urokinase or the proenzyme scuPA, as we have observed in several of our prior reports (18; 20; 21; 23). In addition, the reported murine EMP *S. pneumoniae* model of which we are aware (41) is restricted to 48h survival and is therefore limited with respect to follow up of organizing EMP. The rabbit model therefore is well-positioned for intrapleural administration of human fibrinolysins. These features and the relatively large size of the animals which facilitates reliable intrapleural injection of the IPFT, even when pleural drainage is more difficult, enable testing of the safety and efficacy of IPFT agents used in the clinical setting. The EMP models we now report thereby arguably advance the field.

EMP in rabbits (Figure 2) was associated with increased levels of pleural fluid PAI-1 antigen and activity, which were on average 4-fold greater than those, which we previously found in TCN-induced pleural injury in rabbits (23). The comparability of the increments of PAI-1 in pleural fluids of either *S. pneumoniae* or *P. multocida* infected rabbits suggests that the response may occur in most forms of EMP. Along these lines, the levels of pleural fluid PAI-1 antigen and activity in the rabbits with EMP were comparable to those found in EMP samples from patients enrolled in the MIST2 trial or in those of EMP patients prospectively collected at

UTHSCT. The models therefore recapitulate the relative overexpression of PAI-1 in human EMP, representing another major advantage.

Our study design has limitations in that we used female rabbits of a relatively young age and the literature is likewise limited in its treatment of the impact of these factors on outcomes. In humans, PAI-1 has been identified as a candidate biomarker that correlates with the stage of pediatric EMP and has been offered as an indication for treatment if the value exceeds 1252 ng/ml (5). Notably, increasing levels of intrapleural PAI-1 found in children with EMP (n=57; age 0.3-17 (mean 4.4 y/o) correlated with increasing pleural organization based on sonographic investigation, similar to that used in our study. Intrapleural levels of PAI-1 in pediatric EMP (5) were within the ranges that were observed in pleural fluids of female rabbits (18 months old) with *S. pneumoniae* and *P. multocida* EMP, and in older human patients (median 59 years old, 72% males; (34)) (Figure 2), as well as in prior studies of adult patients with EMP (2; 19; 31; 39). Moreover, the levels of PAI-1 in a group of male patients with EMP (n=44, age 22-85 (median 71) (28) were also comparable to those found in our study (Figure 2). While it appears that pleural disease outcomes and PAI-1 levels may not vary as a function of age or gender, further studies are needed to resolve the question.

Because PAI-1 is increased in EMP (Figure 2) and because rabbit PAI-1 is capable of inhibiting either human scuPA or tPA IPFT (23), the findings strongly suggest that variable levels of PAI-1 activity found in these fluids could have influenced individual outcomes. Based on these data, we speculate that outcomes of tPA-based IPFT in MIST2 could have been affected by variable levels of intrapleural PAI-1 expression (Figure 2) as doses of 10 mg of tPA IPFT with or without DNase were uniformly delivered to each patient (34). Because the quality and amount of DNA in pleural fluids can influence the activity of tPA (26), the same confounder may apply to the tPA/DNase arm of that same trial. The same variability in PAI-1 levels observed in prospectively collected EMP pleural fluids suggests that empiric dosing of

fibrinolysins, now commonly used in clinical practice, could be effective in some patients with relatively lower levels of PAI-1 activity while the same dose may be ineffective in subjects with relatively higher levels. The rabbits inoculated with either *S. pneumoniae* or *P. multocida* exhibited lesser variability of PAI-1 pleural fluid levels than in human EMP (Figure 2), likely related to subtle variations in delivery of the organisms or individual differences in the rabbit's response to pleural infection and inflammation. Notably, an increase in the plasma PAI-1 levels of a similar magnitude in human sepsis correlates with unfavorable outcomes (14; 15; 32; 35; 42), suggesting another possible link between level of PAI-1 and the course of disease (4).

Related to range of pleural fluid levels of PAI-1 activity found in EMP fluids, we also found that dosing of IPFT is critically important in determining outcomes of IPFT in EMP. Intrapleural administration of MED doses of scuPA (proenzyme; 0.5 mg/kg) or tPA (0.145 mg/kg) for TCN-induced pleural injury (27) differed in their ability to clear pleural organization in EMP. In the *S. pneumoniae* EMP model, tPA IPFT at this dose was ineffective (GLIS 50), while scuPA was partially effective. In *P. multocida* EMP, in which pleural fluid PAI-1 concentrations were generally but not significantly higher, tPA and scuPA at the TCN MED doses were ineffective, likely due to generally increased levels of PAI-1 activity (23) or other factors. These agents were given as a single intrapleural dose at the same 72h interval at which time the same doses of either agent were effective in TCN-induced pleural injury. In order to conserve animals, we used the *S. pneumoniae* model alone to test whether delivery of relatively high dose tPA or scuPA was effective and safe in EMP. We found that administration of either tPA or scuPA at 2 mg/kg effectively cleared pleural organization when delivered at 72h, with GLIS scores <10 in all cases (Figure 10E), at 96h demonstrating clear evidence of efficacy. While pleural thickening was not significantly reduced by administration of higher dose; 2 mg/kg scuPA or tPA in either EMP model, there was a trend towards improvement with scuPA IPFT at this dose (Figure 10). These observations confirm those made in the TCN model (23) and unequivocally demonstrate

that increased doses of IPFT are required to clear organizing pleural injury in EMP versus that in TCN-induced pleural injury. By extension, the findings clearly suggest that empiric dosing of IPFT, as has been done in most trials to date, including the MIST 1 and 2 trials, is prone to failed intervention. This contingency raises the possibility of misinterpretation of the efficacy of the agent, rather than of the actual dose of the IPFT that was empirically used.

Tube thoracostomy is generally used in cases of EMP or CPE in which loculation is likely to be chosen in the clinical setting based on biomarker analyses or in cases in which loculation has occurred. However, chest tube placement was not used in the models. This departure from the clinical approach was mandated by our previous experience with chest tube placement in *P. multocida*-induced EMP (20) , in which routine pleural fluid evacuation was needed to ensure survival of the rabbits. We were able to maintain all animals with EMP in this study using round the clock surveillance, which enabled us to study organization of pleural fluid that remains in the chest. In situations in which respiratory distress occurred with increased EMP formation, pleural aspiration was used as needed and subcutaneous sterile saline was administered daily to promote appropriate hydration. Supplemental oxygen was administered as needed to ensure an oxygen saturation of at least 90 percent at all times. These measures were allowed us to carry the model to a period where pleural organization impaired pleural fluid drainage at 72h post infection.

IPFT with either tPA or scuPA was well-tolerated in rabbits with *S. pneumoniae* or *P. multocida*-induced EMP. There was no evidence of pleural or overt systemic bleeding with delivery of either fibrinolysin and both were otherwise well-tolerated, even at a high dose in the *S. pneumoniae* model. While EMP neutrophilia persisted in the *S. pneumoniae* model, a relative predominance of monocytes/macrophages occurred later; by 96h, in *P. multocida*-infected rabbits. EMP total protein and DNA concentrations of EMP fluids did not differ after administration of either tPA or scuPA, indicating that their effects were mainly attributable to

clearance of the fibrinous intrapleural neomatrix as determined by GLIS scoring. At the 2 mg/kg dose, pleural fluid was readily aspirated from the *S. pneumoniae* EMP rabbits, indicated that either agent could enhance the drainage of pleural fluids. Since scuPA is converted to two chain uPA within EMP fluids, it could have enhanced the ease of pleural fluid aspiration as two chain uPA has been shown to decrease the viscosity of pus (30). The inflammatory response within the pleural fluids persisted after clearance of the organisms from the pleural fluids by the antibiotic that was administered for four days after initiation of EMP. This suggests that EMP can progress with organization even after the organism is cleared within pleural fluids.

Processing of scuPA and tPA in pleural fluids in the *S. pneumoniae* and *P. multocida* models was comparable. After administration of scuPA or tPA, detectable fibrinolytic activity in pleural fluids was rapidly quenched as plasminogen was consumed and the fibrinolysins were inhibited by PAI-1, recapitulating the relationship between changes in these components of the fibrinolytic system and the effects of the delivery of scuPA or tPA-based IPFT. Interestingly, pleural fluid fibrinolytic activity was significantly reduced versus levels that occurred in rabbits with EMP treated with either scuPA or tPA (Figures 9, 11C, D) compared ($P<0.05$) to rabbits with TCN-induced injury (13). This observation clearly shows that the processing of either fibrinolysin differs to this extent in EMP and the effects may be due to pleural fluid DNA levels or its quality, replenishment of serpins or differences in levels of plasminogen that may occur. In a previous study, we showed that the PA activity of either two chain uPA or tPA is regulated by the size and quantity of the DNA fragments present in pleural fluids (26). Overall, levels of DNA are increased in pleural fluids of rabbits with EMP, suggesting that IPFT could be altered by the DNA content that may vary in individual subjects.

In a summary, we have reported two rabbit EMP models which recapitulate major features of acute human disease such as accumulation of fibropurulent pleural fluids, followed by loculation and significant pleural thickness, suppression of fibrinolytic and PA activities,

475 accumulation of high levels of endogenous PAI-1, plasminogen and extracellular DNA. We have
476 demonstrated that *S. pneumoniae* EMP in rabbits is successfully treated with 2 mg/kg of tPA, a
477 fibrinolysin, which currently is used for treatment of EMP in adults and scuPA, a proenzyme of
478 urokinase, which is used for treatment of EMP in pediatric patients. In the aggregate, our
479 findings demonstrate that IPFT outcomes are dose-dependent, whether tPA or scuPA is used in
480 the EMP models, in part attributable to variation in the levels of EMP fluid PAI-1 from subject to
481 subject. The clinical ramifications of this study relate to the greater variability of PAI-1 levels in
482 human EMP fluids and the comparable processing of tPA and scuPA within the human and
483 rabbit EMP fluids. Since there is no FDA-approved fibrinolysin for primary IPFT therapy or
484 salvage IPFT for pleural loculation in EMP, dosing of commercially available fibrinolysins is now
485 empiric and off-label dosing regimens may be suboptimal. The findings underscore the need to
486 interpret the results of clinical trials done to date with a keen eye to the dose of fibrinolysin that
487 was used. Our observations suggest the possibility that dose escalation phase I safety trials of
488 IPFT could better define the safety of fibrinolysins used in IPFT, while informing the optimal
489 dosing to be tested for efficacy in phase II clinical trials. Lastly, another ramification of this work
490 is that PAI-1-targeted adjuncts could theoretically reduce the dose of fibrinolysins in IPFT in a
491 manner similar to that we observed in TCN-induced pleural injury in rabbits (13), and thereby
492 increase the safety of this interventional strategy. This postulate remains to be tested in the
493 EMP models we now report.

494
Acknowledgements: The authors are indebted to Dr. W. (Sandy) Hadden (deceased) for his
unparalleled help and support in the creation of the *P. multocida* pleural injury model.

495 496 FOOTNOTES

497 †Abbreviations used are: CPE, Complicated Pleural Effusion; EMP, empyema; GLIS, Gross
498 Lung Injury Score; IPFT, intrapleural fibrinolytic therapy; MED, minimal effective dose; MIST,

499 Multicenter Intrapleural Sepsis Trial; PAI-1, plasminogen activator inhibitor-1; PA, plasminogen
500 activation; RBC, red blood cell; sc, single chain; tc, two chain; TEF, minimal time of effective
501 fibrinolysis; TCN, tetracycline; tPA, tissue type plasminogen activator; uPA, urokinase;
502

Figure Legends

Figure 1. Pleural injury in acute *P. multocida* and *S. pneumoniae* EMP in rabbits. Top panel shows chest ultrasonography (**A**) at 96h after induction of EMP, yellow arrows indicate pleural adhesions seen as rounded opaque structures; L=lung, H=heart; Postmortem visual evaluation (**B**) shows extensive adhesions (black arrows) with fibrinous coating of the lung. Bottom panel shows the histology of pleural injury. Tissue sections were prepared from the lungs of rabbits with *P. multocida* and *S. pneumoniae* induced pleural injury (96h after induction of the model), n= 3 per group. Tissue sections were stained with haematoxylin and eosin, probed for collagen via Trichrome stain and fibrin via immunohistochemistry. The entire sectioned pleura was analyzed for fibrin (red) and collagen (blue) deposition. Arrows indicate fibrin deposition. All images were taken at 20X magnification on a Nikon Eclipse Ti inverted microscope. Illustrated findings are representative of 3 sections/group. Averaged pleural thickness (surface to basement membrane) was 580 and 60 μm for *P. multocida* and *S. pneumoniae*, as determined by morphometry.

Figure 2. Both active and total PAI-1 levels at baseline pleural fluids from rabbits with EMP are similar to those observed in human EMP. A semi-logarithmic plot of concentration (ng/ml) of active (grey) and total (empty) PAI-1 in samples of EMP/CPE pleural fluid (from left to right) from: humans prospectively collected at UTHSCT; patients from the participating in the MIST2 clinical trial; rabbits with *P. multocida* and *S. pneumoniae* induced EMP, respectively. Commercially available ELISAs (Molecular Innovation) were used. Data are presented as box plots (showing interquartile ranges). Results for Kruskal-Wallis test demonstrated no statistically significant difference ($P>0.05$) in the medians either for active PAI-1 or for total antigen among the four groups.

Figure 3. Activation of endogenous plasminogen results in a significant increase in the suppressed fibrinolytic activity in baseline pleural fluids from rabbits with *P. multocida* and *S. pneumoniae* EMP and humans from the MIST2 clinical trials. Aliquots of pleural fluid withdrawn prior to IPFT were analyzed by FITC-fibrin film fibrinolytic activity assay (26) with (empty circles) or without (filled circles) supplementation with 5 nM of tcuPA (13). A significant increase in the baseline fibrinolytic activity occurred after supplementation with exogenous fibrinolysin (empty circles) was observed in pleural fluid samples of (from the left to the right) rabbits with *P. multocida* and *S. pneumoniae*-induced EMP and humans from the MIST2 trials.

Figure 4. Extracellular DNA concentration in pleural fluids of humans and rabbits with EMP. (A) A semi-logarithmic plot of DNA concentration ($\mu\text{g/ml}$) in human (prospectively collected at UTHSCT and MIST2) and rabbit *P. multocida* and *S. pneumoniae*-induced EMP pleural fluids. Total nucleic acids were purified from 100 μl of pleural fluid using a DNeasy blood and tissue kit from Qiagen as described in the manufacturer's protocol. The amounts and size distribution of DNA were estimated by A_{260} **(A)**, and agarose gel electrophoresis **(B)**, where 1- human UTHSCT; 2- human MIST2, 3- rabbit with *P. multocida* EMP, 4- rabbit with *S. pneumoniae* EMP). The reassembly of noncontiguous gel lanes is demarcated by white spaces. Gels were visualized and analyzed using a Molecular Imager supplemented with Quantity One (version 4.2.3) software (Bio-Rad). Data are presented as box plots (showing interquartile ranges). Results for Kruskal-Wallis test presented statistically significant difference in the mean values among the treatment groups ($P < 0.001$). Pairwise multiple comparison showed that the concentration of DNA in the *P. multocida* pleural injury group is statistically higher among the analyzed groups ($P < 0.001$).

Figure 5. The pleural fluids WBC differential counts in rabbit *P. multocida* and *S. pneumoniae* induced pleural injury. Pleural fluids were collected at the time of euthanasia and RBC and WBC count was performed as described in Material and Methods section. A

predominance of neutrophils is noted in *S. pneumoniae* injury while a mixed myeloid cell distribution was seen at 96h after induction of *P. multocida*-induced EMP. Results of paired t-tests showed statistically significant change $p=0.013$ (*) and 0.006 (**) in cell populations. Data are presented as a grouped vertical bar graph.

Figure 6. IPFT with MED of tPA or scuPA identified for TCN-induced rabbit pleural injury (18; 24) was ineffective in treatment of *P. multocida* (A) and *S. pneumoniae* (B) rabbit EMP. (A) Outcomes of IPFT of rabbits with *P. multocida* EMP expressed as GLIS scores (23; 25) for treatment (from the left to the right) with the vehicle (n=5), scuPA (0.5 mg/kg; n=9) and tPA (0.145 mg/kg; n=9). Data are presented as box plots (showing interquartile ranges). Results for Kruskal-Wallis tests showed no statistically significant difference ($P>0.05$) in medians among the treatment groups. **(B)** Outcomes of IPFT of rabbits with EMP for treatment (from left to the right) with vehicle (n=5), scuPA (0.5 mg/kg; n=3) and tPA (0.145 mg/kg; n=3). Data are presented as box plots (showing interquartile ranges). Kruskal-Wallis tests showed no statistically significant difference ($P>0.05$) in medians among the treatment groups.

Figure 7. Unsuccessful IPFT of acute *P. multocida* (top panel) and *S. pneumoniae* (bottom panel) EMP with MED of scuPA or tPA identified for TCN-induced pleural injury (18; 24). Rabbits with acute EMP were treated with 0.5 mg/kg of scuPA or 0.145 mg/kg tPA at 72h (Figure 3). **(A)**; Pleural injury was evaluated at 96h (24 h after IPFT) by gross examination (arrows indicate fibrin depositions and lung coating) and gross findings were confirmed **(B)** by microscopic examination and by immunostaining which showed fibrin (red) on the visceral pleural surface. All images were taken at 20X magnification on a Nikon Eclipse Ti inverted microscope. Illustrated findings are representative of 3 sections/group **(C)**; Pleural thickness (surface to basement membrane) was determined by morphometry (30 fields/slide, n=3 representative sections per animal). Data are presented as box plots (showing interquartile

ranges). Kruskal-Wallis tests showed no statistically significant difference ($P>0.05$) in medians among the treatment groups.

Figure 8. Changes in intrapleural PA activity during IPFT of rabbits with *P. multocida* (A, B) and *S. pneumoniae* (C, D) EMP with scuPA (0.5 mg/kg; A, C) and tPA (0.145 mg/kg; B, D). Changes in enzymatic PA activity in pleural fluids withdrawn at 10, 20, 40 min and at 24h (final) represent kinetics of intrapleural inactivation of scuPA (A,B) and tPA (C, D). PA activity was measured as described in the Materials and Methods and elsewhere (13; 24).

Figure 9. Changes in the fibrinolytic activity in pleural fluids of rabbits with *P. multocida* (A, B) and *S. pneumoniae* (C, D) EMP during IPFT with scuPA (0.5 mg/kg; A, C) and tPA (0.145 mg/kg; B, D). Fibrinolytic activity in pleural fluids withdrawn at 0; 10, 20, 40 min and at the end of the experiment (final) after injection 0.5 mg/kg ($n=3$) scuPA (A, $n=5$; C, $n=3$) or 0.145 mg/kg tPA (B, $n=5$; D, $n=3$). Fibrinolytic activity in aliquots of pleural fluid was measured using a FITC-fibrin film assay as described previously (26).

Figure 10. Effective IPFT of *S. pneumoniae* EMP in rabbits with 2mg/kg of tPA or scuPA clears intrapleural fibrinous adhesions and pleural rind. Rabbits with acute *S. pneumoniae*-induced EMP were treated with 2 mg/kg of scuPA (top row) or tPA (bottom row) at 72h and euthanized at 24h after. **(A)** Chest ultrasonography immediately before IPFT demonstrated extensive opaque pleural adhesions and fibrin deposition (yellow arrows, L-lung, H-heart). **(B)** Chest ultrasonography 8h IPFT demonstrated dissolution of pleural adhesions and fibrin deposition (L-lung, H-heart). Pleural effusion and adhesions were cleared 24h after IPFT as seen on gross examination **(C)**; this was confirmed by immunostaining, which showed very little, focal, fibrin (red) deposition on the visceral pleural surface **(D)**. All images were taken at 40X magnification on a Nikon Eclipse Ti inverted microscope. Illustrated findings are representative of 3 sections/group. **(E)** Outcomes of IPFT were expressed as GLIS (GLIS<10 corresponds to

effective IPFT (13; 25)) for treatment with the vehicle (n=5), scuPA 2 mg/kg (n=5) and tPA 2 mg/kg (n=5). Data are presented as box plots showing interquartile ranges. Kruskal-Wallis tests showed statistically significant differences ($P<0.001$) in medians among the treatment groups.

(F) Pleural thickening (surface to basement membrane) was determined by morphometry (30 fields/slide, n=3 representative sections per animal). Kruskal-Wallis tests did not show statistically significant difference in medians among the treatment groups ($P=0.210$).

Figure 11. Changes in intrapleural PA (A; B) and fibrinolytic (C, D) activities during IPFT of *S. pneumoniae* EMP in rabbits with 2 mg/kg of scuPA (A, C) and tPA (B, D). PA and fibrinolytic activities were determined in pleural fluids of rabbits with *S. pneumoniae*-induced EMP withdrawn at 0; 10, 20, 40 min and at the end of the experiment (24h, final) after injection 2.0 mg/kg of scuPA (n=3; **A, C**) or tPA (n=3; **B, D**). Changes in PA and fibrinolytic activities in pleural fluids withdrawn at the indicated time were measured as described in the Materials and Methods (13; 24).

623

624

Reference List

625

626 1. Abu-Daff S, Maziak DE, Alshehab D, Threader J, Ivanovic J, Deslaurier V,
627 Villeneuve PJ, Gilbert S, Sundaresan S, Shamji F, Lougheed C, Seely JM and Seely
628 AJ. Intrapleural fibrinolytic therapy (IPFT) in loculated pleural effusions--analysis
629 of predictors for failure of therapy and bleeding: a cohort study. *BMJ Open* 3:
630 2013.

631 2. Asselbergs FW, Williams SM, Hebert PR, Coffey CS, Hillege HL, Navis G, Vaughan
632 DE, van Gilst WH and Moore JH. The gender-specific role of polymorphisms from
633 the fibrinolytic, renin-angiotensin, and bradykinin systems in determining plasma
634 t-PA and PAI-1 levels. *Thromb Haemost* 96: 471-477, 2006.

635 3. Bouros D, Antoniou KM, Chalkiadakis G, Drositis J, Petrakis I and Siafakas N. The
636 role of video-assisted thoracoscopic surgery in the treatment of parapneumonic
637 empyema after the failure of fibrinolytics. *Surg Endosc* 16: 151-154, 2002.

638 4. Cesari M, Pahor M and Incalzi RA. Plasminogen activator inhibitor-1 (PAI-1): a key
639 factor linking fibrinolysis and age-related subclinical and clinical conditions.
640 *Cardiovasc Ther* 28: e72-e91, 2010.

641 5. Chiu CY, Wong KS, Huang JL, Tasi MH, Lin TY and Hsieh SY. Proinflammatory
642 cytokines, fibrinolytic system enzymes, and biochemical indices in children with
643 infectious para-pneumonic effusions. *Pediatr Infect Dis J* 27: 699-703, 2008.

6. Chung CL, Chen CH, Sheu JR, Chen YC and Chang SC. Proinflammatory cytokines, transforming growth factor-beta1, and fibrinolytic enzymes in loculated and free-flowing pleural exudates. *Chest* 128: 690-697, 2005.
7. Colice L and Idell S. Counterpoint: should fibrinolytics be routinely administered intrapleurally for management of a complicated parapneumonic effusion? No. *Chest* 145: 17-20, 2014.
8. Colice L and Idell S. Rebuttal from Drs Colice and Idell. *Chest* 145: 21-23, 2014.
9. Declerck PJ, Gils A and De TB. Use of mouse models to study plasminogen activator inhibitor-1. *Methods Enzymol* 499: 77-104, 2011.
10. Decologne N, Kolb M, Margetts PJ, Menetrier F, Artur Y, Garrido C, Gauldie J, Camus P and Bonniaud P. TGF-beta1 induces progressive pleural scarring and subpleural fibrosis. *J Immunol* 179: 6043-6051, 2007.
11. Decologne N, Wettstein G, Kolb M, Margetts P, Garrido C, Camus P and Bonniaud P. Bleomycin induces pleural and subpleural fibrosis in the presence of carbon particles. *Eur Respir J* 35: 176-185, 2010.
12. Dewilde M, Van De CB, Compernelle G, Madsen JB, Strelkov S, Gils A and Declerck PJ. Subtle structural differences between human and mouse PAI-1 reveal the basis for biochemical differences. *J Struct Biol* 2010.

- 662 13. Florova G, Azghani A, Karandashova S, Schaefer C, Koenig K, Stewart-Evans K,
663 Declerck PJ, Idell S and Komissarov AA. Targeting of plasminogen activator
664 inhibitor 1 improves fibrinolytic therapy for tetracycline-induced pleural injury in
665 rabbits. *Am J Respir Cell Mol Biol* 52: 429-437, 2015.
- 666 14. Gando S, Nakanishi Y and Tedo I. Cytokines and plasminogen activator inhibitor-1
667 in posttrauma disseminated intravascular coagulation: relationship to multiple
668 organ dysfunction syndrome. *Crit Care Med* 23: 1835-1842, 1995.
- 669 15. Iba T, Kidokoro A, Fukunaga M, Sugiyama K, Sawada T and Kato H. Association
670 between the severity of sepsis and the changes in hemostatic molecular markers
671 and vascular endothelial damage markers. *Shock* 23: 25-29, 2005.
- 672 16. Idell S. The pathogenesis of pleural space loculation and fibrosis. *Curr Opin Pulm*
673 *Med* 14: 310-315, 2008.
- 674 17. Idell S, Allen T, Chen S, Koenig K, Mazar A and Azghani A. Intrapleural activation,
675 processing, efficacy, and duration of protection of single-chain urokinase in
676 evolving tetracycline-induced pleural injury in rabbits. *Am J Physiol Lung Cell Mol*
677 *Physiol* 292: L25-L32, 2007.
- 678 18. Idell S, Azghani A, Chen S, Koenig K, Mazar A, Kodandapani L, Bdeir K, Cines D,
679 Kulikovskaya I and Allen T. Intrapleural low-molecular-weight urokinase or tissue
680 plasminogen activator versus single-chain urokinase in tetracycline-induced
681 pleural loculation in rabbits. *Exp Lung Res* 33: 419-440, 2007.

19. Idell S, Girard W, Koenig KB, McLarty J and Fair DS. Abnormalities of pathways of fibrin turnover in the human pleural space. *Am Rev Respir Dis* 144: 187-194, 1991.
20. Idell S, Jun NM, Liao H, Gazar AE, Drake W, Lane KB, Koenig K, Komissarov A, Tucker T and Light RW. Single-chain urokinase in empyema induced by *Pasturella multocida*. *Exp Lung Res* 35: 665-681, 2009.
21. Idell S, Mazar A, Cines D, Kuo A, Parry G, Gawlak S, Juarez J, Koenig K, Azghani A, Hadden W, McLarty J and Miller E. Single-chain urokinase alone or complexed to its receptor in tetracycline-induced pleuritis in rabbits. *Am J Respir Crit Care Med* 166: 920-926, 2002.
22. Jo M, Takimoto S, Montel V and Gonias SL. The urokinase receptor promotes cancer metastasis independently of urokinase-type plasminogen activator in mice. *Am J Pathol* 175: 190-200, 2009.
23. Karandashova S, Florova G, Azghani AO, Komissarov AA, Koenig K, Tucker TA, Allen TC, Stewart K, Tvinnereim A and Idell S. Intrapleural adenoviral delivery of human plasminogen activator inhibitor-1 exacerbates tetracycline-induced pleural injury in rabbits. *Am J Respir Cell Mol Biol* 48: 44-52, 2013.
24. Komissarov AA, Florova G, Azghani A, Karandashova S, Kurdowska AK and Idell S. Active alpha-macroglobulin is a reservoir for urokinase after fibrinolytic therapy in rabbits with tetracycline-induced pleural injury and in human pleural fluids. *Am J Physiol Lung Cell Mol Physiol* 305: L682-L692, 2013.

- 702 **25. Komissarov AA, Florova G, Azghani AO, Buchanan A, Bradley WM, Schaefer C,**
703 **Koenig K and Idell S. The time course of resolution of adhesions during**
704 **fibrinolytic therapy in tetracycline-induced pleural injury in rabbits. *Am J Physiol***
705 ***Lung Cell Mol Physiol* 309: L562-L572, 2015.**
- 706 **26. Komissarov AA, Florova G and Idell S. Effects of extracellular DNA on**
707 **plasminogen activation and fibrinolysis. *J Biol Chem* 286: 41949-41962, 2011.**
- 708 **27. Komissarov AA, Mazar AP, Koenig K, Kurdowska AK and Idell S. Regulation of**
709 **intrapleural fibrinolysis by urokinase-alpha-macroglobulin complexes in**
710 **tetracycline-induced pleural injury in rabbits. *Am J Physiol Lung Cell Mol Physiol***
711 **297: L568-L577, 2009.**
- 712 **28. Lin FC, Chen YC, Chen FJ and Chang SC. Cytokines and fibrinolytic enzymes in**
713 **tuberculous and parapneumonic effusions. *Clin Immunol* 2005.**
- 714 **29. Midde KK, Batchinsky AI, Cancio LC, Shetty S, Komissarov AA, Florova G, Walker**
715 **KP, III, Koenig K, Chroneos ZC, Allen T, Chung K, Dubick M and Idell S. Wood bark**
716 **smoke induces lung and pleural plasminogen activator inhibitor 1 and stabilizes**
717 **its mRNA in porcine lung cells. *Shock* 36: 128-137, 2011.**
- 718 **30. Park JK, Kraus FC and Haaga JR. Fluid flow during percutaneous drainage**
719 **procedures: an in vitro study of the effects of fluid viscosity, catheter size, and**
720 **adjunctive urokinase. *AJR Am J Roentgenol* 160: 165-169, 1993.**

- 721 31. Philip-Joet F, Alessi MC, Philip-Joet C, Aillaud M, Barriere JR, Arnaud A and
722 Juhan-Vague I. Fibrinolytic and inflammatory processes in pleural effusions. *Eur*
723 *Respir J* 8: 1352-1356, 1995.
- 724 32. Pralong G, Calandra T, Glauser MP, Schellekens J, Verhoef J, Bachmann F and
725 Kruithof EK. Plasminogen activator inhibitor 1: a new prognostic marker in septic
726 shock. *Thromb Haemost* 61: 459-462, 1989.
- 727 33. Pretorius E, Humphries P, Ekpo OE, Smit E and van der Merwe CF. Comparative
728 ultrastructural analyses of mouse, rabbit, and human platelets and fibrin
729 networks. *Microsc Res Tech* 70: 823-827, 2007.
- 730 34. Rahman NM, Maskell NA, West A, Teoh R, Arnold A, Mackinlay C, Peckham D,
731 Davies CW, Ali N, Kinnear W, Bentley A, Kahan BC, Wrightson JM, Davies HE,
732 Hooper CE, Lee YC, Hedley EL, Crosthwaite N, Choo L, Helm EJ, Gleeson FV,
733 Nunn AJ and Davies RJ. Intrapleural Use of Tissue Plasminogen Activator and
734 DNase in Pleural Infection. *N Engl J Med* 365: 518-526, 2011.
- 735 35. Semeraro N, Ammollo CT, Semeraro F and Colucci M. Sepsis, thrombosis and
736 organ dysfunction. *Thromb Res* 129: 290-295, 2012.
- 737 36. Thommi G, Nair CK, Aronow WS, Shehan C, Meyers P and McLeay M. Efficacy and
738 safety of intrapleural instillation of alteplase in the management of complicated
739 pleural effusion or empyema. *Am J Ther* 14: 341-345, 2007.

740 37. Tillett WS and Sherry S. The effect in patients of streptococcal fibrinolysin
741 (streptokinase) and streptococcal desoxyribonuclease on fibrinous, purulent and
742 sanguinous pleural exudations. *J Clin Invest* 28, 173-190. 1949.

743 Ref Type: Generic

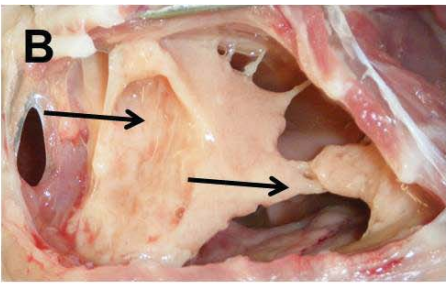
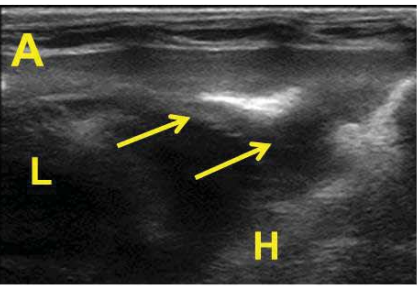
744 38. Tillett WS, Sherry S. and Read CT. The use of streptokinase-streptodornase in the
745 treatment of postpneumonic empyema. *J Thorac Surg* 21: 275-297, 1951.

746 39. Tofler GH, Massaro J, Levy D, Mittleman M, Sutherland P, Lipinska I, Muller JE and
747 D'Agostino RB. Relation of the prothrombotic state to increasing age (from the
748 Framingham Offspring Study). *Am J Cardiol* 96: 1280-1283, 2005.

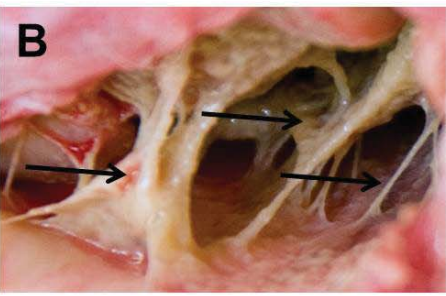
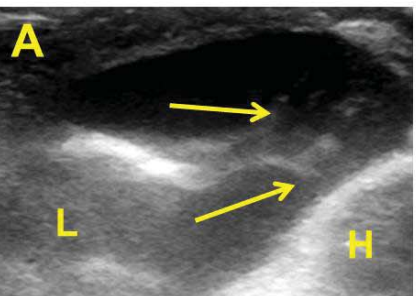
749 40. Tucker T and Idell S. Plasminogen-plasmin system in the pathogenesis and
750 treatment of lung and pleural injury. *Semin Thromb Hemost* 39: 373-381, 2013.

751 41. Wilkosz S, Edwards LA, Bielsa S, Hyams C, Taylor A, Davies RJ, Laurent GJ,
752 Chambers RC, Brown JS and Lee YC. Characterization of a new mouse model of
753 empyema and the mechanisms of pleural invasion by *Streptococcus pneumoniae*.
754 *Am J Respir Cell Mol Biol* 46: 180-187, 2012.

755 42. Zeerleder S, Schroeder V, Hack CE, Kohler HP and Willemin WA. TAFI and PAI-1
756 levels in human sepsis. *Thromb Res* 118: 205-212, 2006.



P. multocida

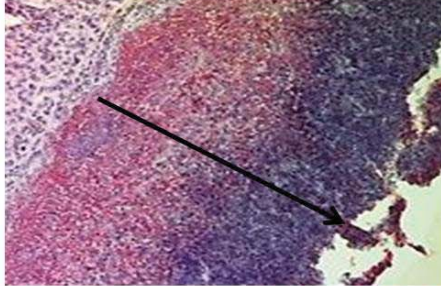
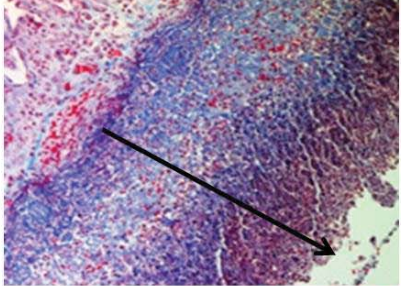
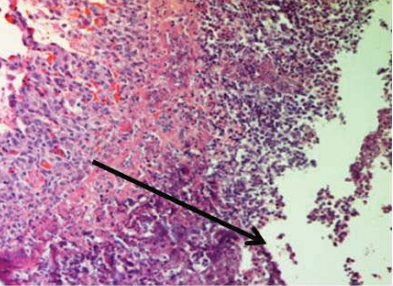


S. pneumoniae

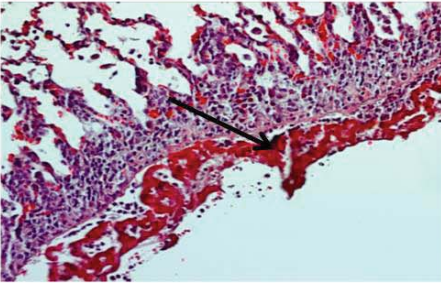
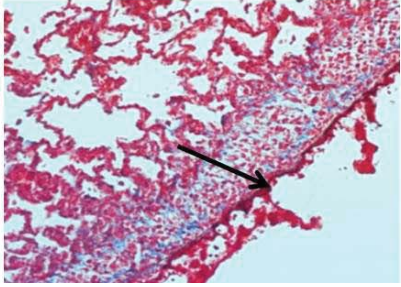
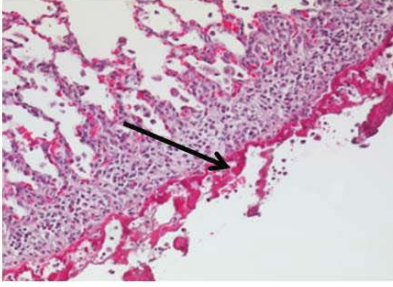
H&E

Trichrome

Fibrin



P. multocida



S. pneumoniae

